

# Orbital analysis of the satellite formation establishment for the ITASAT#2 mission

Caio Nahuel Sousa Fagonde<sup>1</sup>, Thais Cardoso Franco<sup>2</sup>, Antonio Fernando Bertachini de Almeida Prado<sup>3</sup> e Willer Gomes dos Santos<sup>2</sup>

<sup>1</sup>Universidade Federal do ABC, Santo André/São Paulo - Brasil

<sup>2</sup>Instituto Tecnológico de Aeronáutica, São José dos Campos/São Paulo - Brasil

<sup>3</sup>Instituto Nacional de Pesquisas Espaciais, São José dos Campos/São Paulo - Brasil

**Abstract**—The ITASAT#2 mission is an upcoming nanosatellite mission that aims to investigate ionospheric plasma bubbles and performs geolocation studies using three formation flying CubeSats. Formation flying missions often have strict constraints on the geometric configuration of the satellites' relative state. In order for the CubeSats to correctly achieve their desired spatial distribution, the acquisition, or establishment phase of the mission must be carefully planned and carried out. With this in mind, the current work aims to analyze the preliminary  $\Delta V$  budget required for the establishment phase of two possible formation configurations: the co-orbital String of Beads and the Non-coplanar Oscillator. In order to do so, the necessary phasing and out-of-plane maneuvers were analyzed and simulated.

**Keywords**—CubeSat, Formation Flying, ITASAT#2.

## I. INTRODUCTION

The upcoming ITASAT#2 mission will be composed of three formation flying CubeSats, with an expected launch window to occur during the solar activity maximum between the years of 2024 and 2026. It will operate with three main objectives: geolocation of signals emitted from a source on the ground via triangulation, using methods such as *Frequency Difference of Arrival* (FDOA) and *Time Difference of Arrival* (TDOA)[1]; in-situ monitoring of the ionosphere, focusing on studying the plasma bubbles that form at altitudes of around 370 km [2]; and technological demonstration of formation flying capabilities.

Much like many of the previous formation flying missions preceding it [3], the ITASAT#2 mission will have a strong focus on a technological demonstration for the coordinated guidance, navigation, and control of spacecraft. The inter-satellite relative states have a strong impact on geolocation accuracy, and so maintenance of their precise configuration is essential for the accomplishment of geolocation services.

The study of ionospheric phenomena and anomalies, on the other hand, is of great significance for preserving the integrity and efficacy of communication infrastructure, such as *GPS* signal processing, since accurate models of the ionosphere and ionospheric plasma do not yet exist for the Brazilian geospatial region. As such, the mission will be a continuation of ongoing efforts in the ionospheric modeling, such as those of the SPORT mission [4], with the overall aim of improving scientific understanding of the ionospheric environment, with a particular interest in the equatorial plasma bubbles that form from sunset electrodynamic processes [5].

Previous and ongoing space missions that involve a long-term coordinated flight of satellites include the Israeli

*SAMSON* project, which consists of a cluster of three CubeSats that aim to demonstrate geolocation capabilities [6]; the TanDEM-X/TerraSAR-X mission, which demonstrated formation flying as a means of creating a distributed Synthetic Aperture Radar [7]; the Magnetospheric Multiscale (MMS) mission used four spacecraft flying in a tetrahedral formation to study magnetic reconnection in the magnetosphere [8]; and the upcoming Small-scale Magnetosphere and Ionosphere Plasma Experiment (SNIPE), which also intends to use four formation-flying satellites to study ionospheric phenomena [9].

In this context, the current work builds on previous studies [2][10] to aid in the development of the orbital analysis for the ITASAT#2 mission. This article is organized as follows: a brief introduction to Spacecraft Formation Flying is presented, followed by explanations of the two configurations considered in this study. Afterward, the methods used for maneuver analysis are detailed, and finally, the results of the simulations are presented and discussed.

### A. Spacecraft Formation Flying

Spacecraft Formation Flying is a rapidly-developing field of interest in space applications, allowing for a group of smaller satellites to act in unison to perform the role that would have been previously relegated to large, monolithic satellites.

More rigorously, it can be defined as the coordinated flight of a group of spacecraft whose dynamic states are linked by a common control law [11].

This allows for greatly reduced costs in mission development while adding dynamical complexity to the system. For any specific mission, the satellites' configuration, also called their *topology*, must be carefully chosen in order to mitigate natural perturbations and achieve the relative motion that is best suited for the mission's goals. Coordination approaches of each topology can be divided into three main categories [12]:

- 1) Leader/Follower approaches, where one satellite is designated as the leader, and the followers have their relative motion described in relation to it.
- 2) Orbital tracking, where each satellite's orbit is tracked individually.
- 3) Virtual structures, similar to a Leader/Follower approach, but with a virtual (fictitious) satellite as the leader.

In this study, two topologies are presented and analyzed for the ITASAT#2 mission: the co-orbital String of Beads and

the Non-coplanar Oscillator. Both follow an Orbital-Tracking coordination approach, as their relative motion requirements are simple and can be more easily described by analyzing the absolute orbital motion of each satellite.

1) *Co-orbital String of Beads*: In this topology, each satellite lies on the same orbit, with a small separation in the mean anomaly. This formation is advantageous for studying the atmospheric plasma bubbles, but it creates a direction of collinearity along with the orbital motion, making it impractical for achieving the mission's geolocation objectives [10]. An example of this configuration can be seen in Fig. 1, with each colored dot representing a satellite.



Fig. 1. Representation of a String of Beads configuration.

2) *Non-coplanar oscillator*: This formation is similar to the String of Beads, but one of the satellites has a slightly different orbital plane, with a small variation in its Right Ascension of Ascending Node (RAAN), exemplified in Fig. 2, where one can see that there are two satellites in the same orbital track, and one offset satellite. This allows for easier triangulation of objects, making it a good formation for geolocation [10].

Since only the RAAN of the off-plane satellite is changed, their relative orbits will be  $J_2$ -invariant in regard to the other two satellites, minimizing perturbations due to zonal effects of the Earth's oblateness [13].



Fig. 2. Representation of a Non-coplanar configuration.

## II. METHODOLOGY

Following orbital deployment and the initial commissioning phase, each satellite must be maneuvered to their desired

stations in order to accomplish the mission's goals. This phase is referred to as the formation establishment phase.

The orbital maneuvers that must be carried out in order to establish a specific formation depend on the final desired configuration. For the String of Beads, only in-plane maneuvering is needed, while the Non-coplanar formation requires a change to the orbital plane of at least one satellite, in order to achieve the desired difference in RAAN.

In this section, the methods used to model the establishment of each topology will be presented.

### A. Establishment of a co-orbital formation

The establishment of a String of Beads mainly entails obtaining the desired angular difference between each satellite, also referred to as a phase difference. Establishing this difference involves repositioning the satellites along the same orbit, which can be achieved by slightly altering the satellite's semimajor axis, and therefore changing the satellite's angular velocity. This type of maneuver is known as a phasing maneuver. Since small satellites often have to work with low-thrust propulsion due to physical and operational constraints, a continuous-thrust formulation is required for the orbital maneuvers, rather than an impulsive one.

The methodology for the continuous-thrust phasing used in this study is based on the simplified analytical model presented in [14]. The main assumptions underlying this model are that the orbits are near-circular and that the altitude does not vary considerably during the maneuver. These assumptions are satisfied by long maneuvering periods, which allow for smaller required acceleration values.

The thrust necessary to achieve a given final angular separation of  $\Delta M$  over a maneuvering period of  $\Delta T$  depends on the thrusting period,  $t_1$ , during which the satellite will experience a tangential maneuvering acceleration, given by Eq. (1), where  $r_0$  is the satellite's initial orbital radius:

$$a_c = -\frac{r_0 \Delta M}{3t_1(\Delta T - t_1)}. \quad (1)$$

After this initial thrusting period, the maneuvering satellite undergoes a coasting period, during which the angular separation changes according to the difference in angular velocity. Finally, a second thrusting period re-inserts the satellite back into its original orbit. Figure 3 illustrates the overall phasing procedure, where  $\Delta M_f$  is the final achieved separation in the mean anomaly.

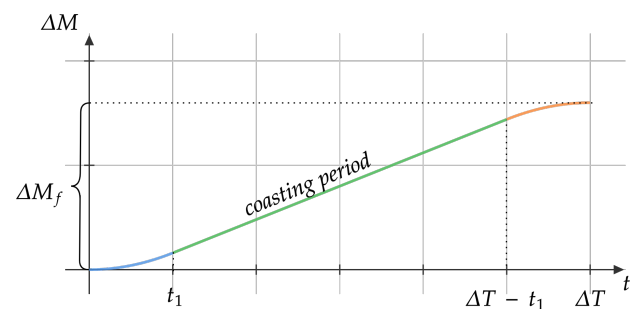


Fig. 3. Visualization of the phasing maneuver.

The total  $\Delta V$  for the phasing maneuver is given by Eq. (2):

$$\Delta V = \frac{2}{3} \frac{r_0 \Delta M}{(\Delta T - t_1)}. \quad (2)$$

And the required  $\Delta M$  necessary to achieve a specified inter-satellite separation ( $\Delta S$ ) varies with the semimajor axis ( $a_0$ ), as shown in Eq. (3):

$$\Delta M = \pm 2 \arcsin \left( \frac{\Delta S}{2a_0} \right). \quad (3)$$

### B. Establishment of a Non-coplanar Oscillator formation

The Non-coplanar Oscillator (NCO) formation requires both phasing and an out-of-plane transfer in order to place the offset-satellite in its station, with a difference in the RAAN ( $\Omega$ ) in regard to the initial orbit.

Reference [15] provides two ways to induce a change in the RAAN: continuous out-of-plane thrusting, switching directions at the line of nodes, or transferring to a drift orbit where the difference in the natural rate of nodal precession will result in the desired change in the non-coplanar orbit. For the first scenario, the  $\Delta V$  expenditure can be estimated as indicated by Eq. (4), where  $\mu$ ,  $a_0$ ,  $i_0$ , and  $\Delta\Omega$  are the Earth's gravitational parameter, the satellite's semimajor axis, the reference orbit's inclination, and the desired change in RAAN, respectively:

$$\Delta V = \frac{\pi}{2} \sqrt{\frac{\mu}{a_0}} \sin i_0 |\Delta\Omega|. \quad (4)$$

The required  $\Delta\Omega$  depends on the desired inter-satellite separation. Reference [10] provides a way to calculate this offset, reproduced in Eq. (5):

$$\Delta\Omega = 2 \arcsin \left( \frac{\Delta S}{2a_0} \right). \quad (5)$$

And the required difference in mean anomaly, considering a circular orbit, is given by:

$$\Delta M = \Delta S \cdot K_{NCO}. \quad (6)$$

Where the constant factor  $K_{NCO}$  depends on orbital altitude and inclination. For an inclination and altitude of  $i_0 = 50^\circ$  and  $h_0 = 400$  km, respectively, its value is:

$$K_{NCO} = 0.185 \text{ s} \cdot \text{km}^{-1}.$$

In the second method, the difference in RAAN is generated by exploiting natural perturbations caused by the Earth's oblateness. This perturbation is represented by the  $J_2$  zonal term of the spherical harmonics representation of the Earth's gravitational potential.

The secular variation of  $\Omega$  under the influence of  $J_2$  is given in Eq. (7) for the circular-orbit case, where  $R_e$  is the Earth's equatorial radius [16].

$$\dot{\Omega} = -\frac{3R_e^2 J_2}{2} \sqrt{\frac{\mu}{a_0^3}} \cos i_0. \quad (7)$$

And so an intermediary *drift orbit* can be established, by varying either the semimajor axis or the inclination of the satellite with regard to the reference orbit, resulting in a differential rate of nodal precession. This may be expressed as the difference between rates of the satellites:

$$\delta\dot{\Omega} = \dot{\Omega}_{offset} - \dot{\Omega}_1. \quad (8)$$

Equation (8) allows for the computation of the necessary change in semimajor axis or inclination required to achieve a given  $\delta\dot{\Omega}$ , knowing the precession rate for the initial reference orbit,  $\dot{\Omega}_1$ . In this study, only a change in inclination was considered for the establishment of the drift orbit, in order to keep the satellites' mean motion unchanged.

Furthermore, in order to achieve better fuel balancing between all satellites, the effort in establishing the drift orbit can be mitigated by having all the satellites change their inclination simultaneously, rather than a single one. This second approach will be referred to as a "shared maneuver". If  $\delta i$  is the change in inclination required for a given differential nodal precession rate, then Eq. (8) may be rewritten as:

$$\delta\dot{\Omega} = -\frac{3R_e^2 J_2}{2} \sqrt{\frac{\mu}{a_0^3}} \left[ \cos(i_0 + \delta i) - \cos(i_0 - \delta i) \right]. \quad (9)$$

This expression can be further simplified as:

$$\delta\dot{\Omega} = 3R_e^2 J_2 \sqrt{\frac{\mu}{a_0^3}} \sin i_0 \sin \delta i. \quad (10)$$

With the value for the required change in inclination, the  $\Delta V$  cost for establishing the drift orbit can then be calculated in the continuous-thrust case as [17]:

$$\Delta V = \sqrt{\frac{\mu}{a_0}} \sqrt{2 - 2 \cos \left( \frac{\pi}{2} \delta i \right)}. \quad (11)$$

## III. RESULTS

The numerical simulations performed focused mainly on investigating the effects of parameter variation on the final  $\Delta V$  for each type of maneuver: in-plane phasing and out-of-plane transfers.

For all phasing maneuvers, the total maneuvering time was arbitrarily chosen to range from 1 to 10 days, with the thrust firing duration ranging from 10% to 50% of the orbital period (T). For the differential nodal precession-based plane change, the main parameter considered was the drift period, ranging from 30 days to 2 years.

In order to calculate the desired phase and RAAN differences, the separation  $\Delta S$  must first be set. Table I lists the desired inter-satellite separation for each of the two topologies, based on the results of [10] for optimal geolocation performance.

TABLE I  
INTER-SATELLITE SEPARATION

Topology	Separation
Co-orbital	343.5 km
Non-coplanar Oscillator	649 km

Table II presents the orbital parameters used in the simulations, where  $h_0$ ,  $e_0$ ,  $i_0$ ,  $\omega_0$ , and  $\Omega_0$  are the orbital altitude, eccentricity, inclination, argument of perigee, and RAAN, respectively.

For the orbital propagation, the  $J_2$  zonal term was taken into account, and the satellites were assumed to be initially coincidental.

TABLE II  
 SIMULATION PARAMETERS

Parameter	Value
$h_0$	370 km
$e_0$	0
$i_0$	51.64°
$\omega_0$	0°
$\Omega_0$	0°

### A. String of Beads

Figures 4 and 5 show the results of the corresponding  $\Delta V$  and acceleration required for the phasing maneuver, represented by the color bars, as a function of the maneuver time and the thrust firing duration. The chosen maneuvering time was the main driver in  $\Delta V$  consumption, with longer maneuvering times leading to smaller required thrust and  $\Delta V$ , which can be seen from the fact that the region with the highest  $\Delta V$  is in the left-most region of the graph, indicated by a yellow color. Overall, the  $\Delta V$  was no higher than 3 m/s for the range of values considered.

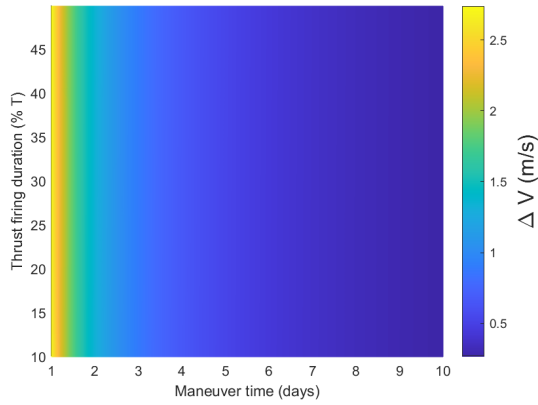


Fig. 4. Simulation results, showing the effects of the maneuver time  $\Delta T$  and thrusting period  $t_1$  on the required  $\Delta V$ .

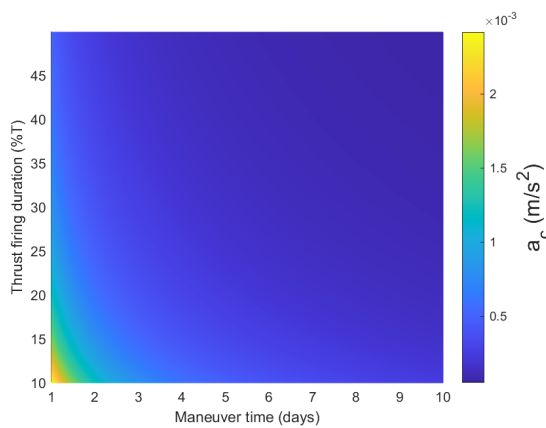


Fig. 5. Simulation results, showing the effects of the maneuver time  $\Delta T$  and thrusting period  $t_1$  on the required acceleration  $a_c$ .

Figure 6 shows the final separation obtained after simulating the phasing maneuver using the analytical method presented. It is clear that using this methodology, longer maneuvering times guarantee more accurate results, closer to the desired separation of 343.5 km, indicated by the horizontal line.

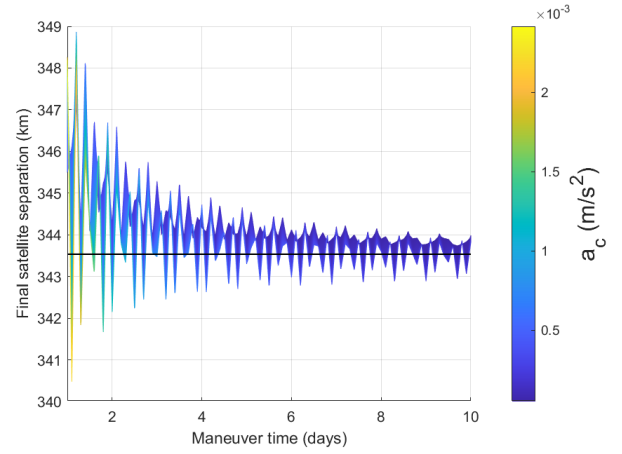


Fig. 6. Simulation results, showing the effects of the maneuver time  $\Delta T$  on the final achieved separation  $\Delta S$ .

### B. Non-coplanar Oscillator

Analysis of the NCO formation's establishment was divided between the in-plane phasing maneuver and the out-of-plane maneuver.

1) *Phasing maneuver:* The phasing maneuver requirements for the NCO formation differ between both maneuvering satellites. The offset satellite has a corresponding desired phase difference given by Eq. (5), which leads to a smaller required mean anomaly difference in comparison to the co-orbital maneuvering satellite.

Figures 7 and 8 show the resulting  $\Delta V$  and required acceleration for the phasing maneuver of the offset satellite. The phasing  $\Delta V$  for the offset satellite is low, due to a smaller required phase difference.

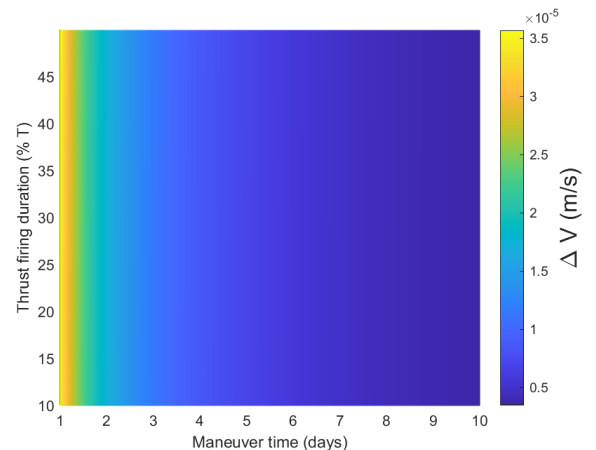


Fig. 7.  $\Delta V$  requirements for the phasing maneuver of the offset satellite.

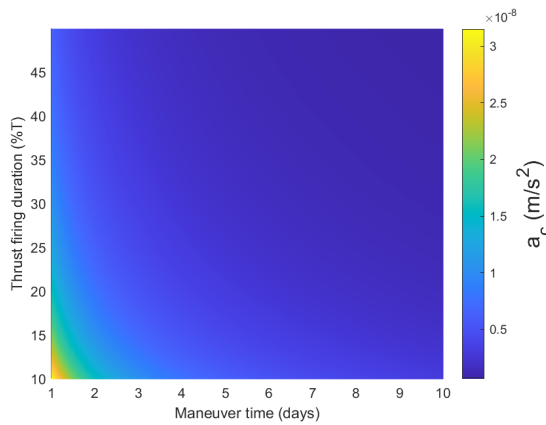


Fig. 8. Acceleration requirements for the phasing maneuver of the offset satellite.

Figures 9 and 10 show the resulting  $\Delta V$  and required acceleration for the phasing maneuver of the co-orbital satellite. While the  $\Delta V$  values associated with the phasing maneuver of the co-orbital satellite are higher, they do not exceed 6 m/s.

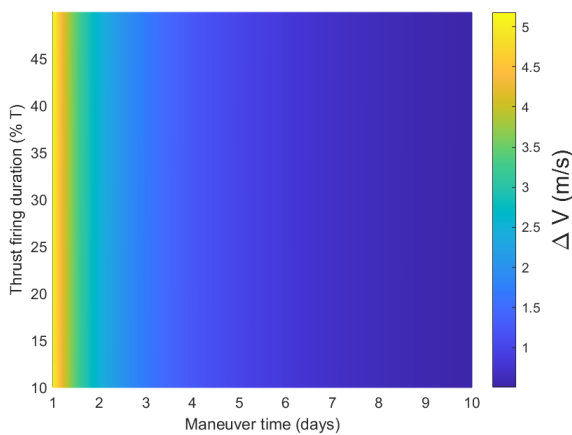


Fig. 9.  $\Delta V$  requirements for the phasing maneuver of the co-orbital satellite.

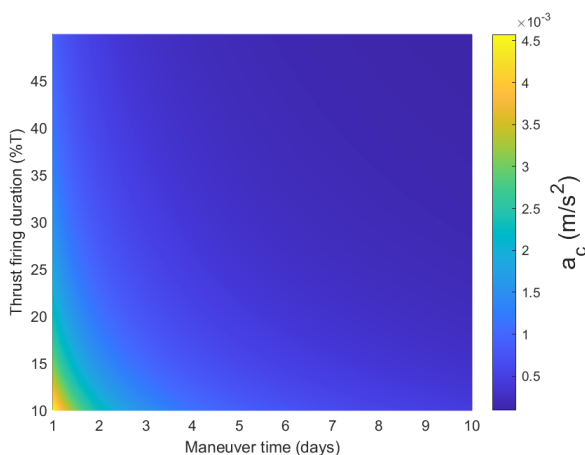


Fig. 10. Acceleration requirements for the phasing maneuver of the co-orbital satellite.

2) *Out-of-plane transfer*: Generating the necessary change to the orbital plane of the offset satellite via propulsive means

is prohibitively costly in terms of the required  $\Delta V$ , resulting in a required change in velocity of around 900 m/s.

For the case of establishment of a drift orbit for the differential nodal precession-based plane establishment, Figures 11 and 12 show the correspondence between allowed drift time and the required  $\Delta V$  for establishing the drift orbit, for the single-maneuvering satellite and the shared maneuver cases, respectively. Each color bar represents the change in inclination needed to achieve the drift orbit.

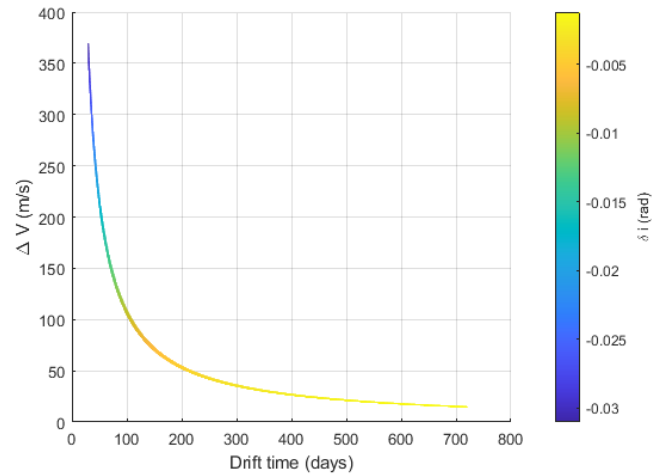


Fig. 11.  $\Delta V$  requirements for establishing the drift orbit.

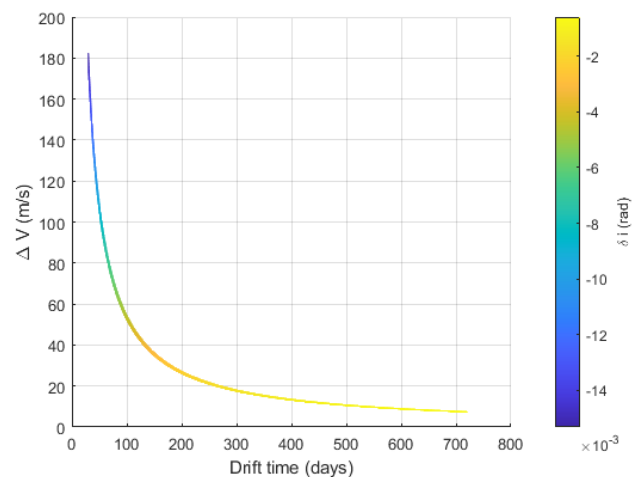


Fig. 12.  $\Delta V$  requirements for establishing the drift orbit using a shared maneuver.

Considering a maximum acceptable drift time of one year, Figures 13 and 14 show the required  $\Delta V$  for the establishment of the drift orbit, for the single-maneuvering satellite and shared maneuver cases. The corresponding values of 28.9 m/s and 14.4 m/s show that the maneuvering costs can be essentially cut in half by performing a shared maneuver.

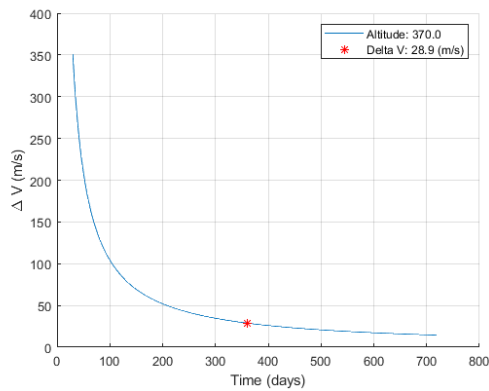


Fig. 13.  $\Delta V$  requirements for a one-year drift orbit.

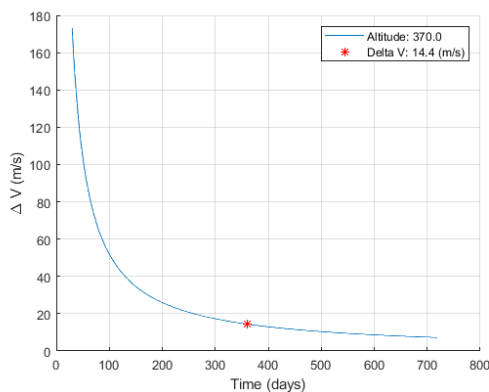


Fig. 14.  $\Delta V$  requirements for a one-year drift orbit based on a shared maneuver.

#### IV. CONCLUSION

In this study, the establishment of two formation topologies for the ITASAT#2 mission, the String of Beads and the Non-coplanar Oscillator, were analyzed in terms of the required orbital maneuvers.

The phasing maneuver, required by both topologies, was shown to be not considerably expensive in terms of  $\Delta V$  expenditure, with it depending mainly on the allowed maneuvering time: longer maneuvering periods led to lower  $\Delta V$  and thrust requirements.

The non-coplanar transfer required by the NCO formation was found to be prohibitively costly if performed via propulsive means, requiring upwards of 900 m/s of  $\Delta V$ . However, it was also shown how this cost may be mitigated by exploiting natural perturbations caused by the Earth's oblateness: establishment of a drift orbit in which the differential nodal precession will naturally lead to the desired difference in RAAN can cut down the required cost, especially when the shared maneuver approach is used. The main fuel-consumption driver, in this case, is the allowed drift time, with short periods leading to an exponentially higher cost for the establishment of the drift orbit, since the corresponding inclination change becomes larger.

A proposal for future work involves the optimization of the drift orbit for  $\Delta V$  minimization, with simultaneous changes to the semimajor axis and inclination, and incorporation of other perturbations, such as differential drag and solar radiation pressure as a means of controlling the relative maneuvering of the satellites.

#### V. ACKNOWLEDGMENT

The authors would like to thank the Aeronautics Institute of Technology ("Instituto Tecnológico de Aeronáutica" - ITA) and the Coordination for the Improvement of Higher Education Personnel ("Coordenação de Aperfeiçoamento de Pessoal de Nível Superior" - CAPES), which finances the subscriptions to journals in the ITA library, as well as the E<sup>2</sup>MoC research group (CNPq certification number 466157) for their support.

#### REFERENCES

- [1] Y. Cao, L. Peng, J. Li, L. Yang, and F. Guo, "A new iterative algorithm for geolocating a known altitude target using TDOA and FDOA measurements in the presence of satellite location uncertainty," *Chinese Journal of Aeronautics*, vol. 28, no. 5, pp. 1510–1518, 2015.
- [2] T. C. Franco and W. G. dos Santos, "ITASAT-2: Formation flying maneuver and control considering J2 disturbances and differential drag," in *SIMPÓSIO DE APLICAÇÕES OPERACIONAIS EM ÁREAS DE DEFESA - SIGE*, 2020.
- [3] S. Bandyopadhyay, R. Foust, G. P. Subramanian, S.-J. Chung, and F. Y. Hadaegh, "Review of formation flying and constellation missions using nanosatellites," *Journal of Spacecraft and Rockets*, vol. 53, no. 3, pp. 567–578, 2016.
- [4] J. Spann, C. Swenson, O. Durao, L. Loures, R. Heelis, R. Bishop, G. Le, M. Abdu, L. Krause, C. Fry *et al.*, "The scintillation prediction observations research task (SPORT): an international science mission using a cubesat," in *31st Annual AIAA/USU Small Satellite Conference*, 2017.
- [5] M. Abdu, I. Batista, A. Carrasco, and C. Brum, "South Atlantic magnetic anomaly ionization: A review and a new focus on electrodynamic effects in the equatorial ionosphere," *Journal of Atmospheric and Solar-Terrestrial Physics*, vol. 67, no. 17-18, pp. 1643–1657, 2005.
- [6] P. Gurfil, J. Herscovitz, and M. Pariente, "SSC12-VII-2 The SAMSON Project – Cluster Flight and Geolocation with Three Autonomous Nano-satellites," in *Proceedings of the AIAA/USU Conference on Small Satellites*, 2012.
- [7] T. Esch, H. Taubenböck, A. Roth, W. Heldens, A. Felbier, M. Schmidt, A. A. Mueller, M. Thiel, and S. W. Dech, "TanDEM-X mission-new perspectives for the inventory and monitoring of global settlement patterns," *Journal of Applied Remote Sensing*, vol. 6, no. 1, p. 061702, 2012.
- [8] S. Fuselier, W. Lewis, C. Schiff, R. Ergun, J. Burch, S. Petrinec, and K. Trattner, "Magnetospheric multiscale science mission profile and operations," *Space Science Reviews*, vol. 199, no. 1, pp. 77–103, 2016.
- [9] Y. Song, S.-Y. Park, S. Lee, P. Kim, E. Lee, and J. Lee, "Spacecraft formation flying system design and controls for four nanosats mission," *Acta Astronautica*, 2021.
- [10] L. M. d. Santos, "Estudo de topologias de formação em voo para uma missão espacial de geolocalização composta por três satélites cubesats," Master's thesis, Instituto Nacional de Pesquisas Espaciais (INPE), São José dos Campos, 2021-03-26. [Online]. Available: <http://urlib.net/rep/8JMKD3MGP3W34T/44STEG5>
- [11] D. P. Scharf, F. Y. Hadaegh, and S. R. Ploen, "A survey of spacecraft formation flying guidance and control. part ii: control," in *Proceedings of the 2004 American control conference*, vol. 4. IEEE, 2004, pp. 2976–2985.
- [12] K. Alfriend, S. R. Vadali, P. Gurfil, J. How, and L. Breger, *Spacecraft formation flying: Dynamics, control and navigation*. Elsevier, 2009, vol. 2.
- [13] D. CaJacob, N. McCarthy, T. O'Shea, and R. McGwier, "Geolocation of RF Emitters with a Formation-Flying Cluster of Three Microsatellites," in *30th Annual AIAA/USU Small Satellite Conference*, 2016.
- [14] M. Martínez-Sánchez and P. Lozano. (2015, Spring) Space propulsion. Massachusetts Institute of Technology: MIT OpenCourseWare. [Online]. Available: <https://ocw.mit.edu>
- [15] J. Pollard, "Simplified Analysis of Low-Thrust Orbital Maneuvers," The Aerospace Corporation, Tech. Rep., 2000.
- [16] C. N. McGrath and M. Macdonald, "General perturbation method for satellite constellation deployment using nodal precession," *Journal of Guidance, Control, and Dynamics*, vol. 43, no. 4, pp. 814–824, 2020.
- [17] A. Ruggiero, P. Pergola, S. Maruccio, and M. Andrenucci, "Low-thrust maneuvers for the efficient correction of orbital elements," in *32nd International Electric Propulsion Conference*, 2011, pp. 11–15.